IOPscience iopscience.iop.org

Home Search Collections Journals About Contact us My IOPscience

A metallization and bonding approach for high performance carbon nanotube thermal interface materials

This article has been downloaded from IOPscience. Please scroll down to see the full text article.

2010 Nanotechnology 21 445705

(http://iopscience.iop.org/0957-4484/21/44/445705)

View the table of contents for this issue, or go to the journal homepage for more

Download details:
IP Address: 143.215.23.194
The article was downloaded on 03/08/2012 at 14:05

Please note that terms and conditions apply.

Nanotechnology **21** (2010) 445705 (8pp) doi:10.1088/0957-4484/21/44/445705

A metallization and bonding approach for high performance carbon nanotube thermal interface materials

Robert Cross[1], Baratunde A Cola[2], Timothy Fisher[2], Xianfan Xu[2], Ken Gall[3] and Samuel Graham[1,3]

[1] George W Woodruff School of Mechanical Engineering, Georgia Institute of Technology, 771 Ferst Drive, Atlanta, GA 30332, USA
[2] Birck Nanotechnology Center, Purdue University, 1205 W State Street, West Lafayette, IN 47907, USA
[3] School of Materials Science and Engineering, Georgia Institute of Technology, 771 Ferst Drive, Atlanta, GA 30332, USA

E-mail: sgraham@gatech.edu

Received 17 March 2010, in final form 26 August 2010
Published 8 October 2010
Online at stacks.iop.org/Nano/21/445705

Abstract
A method has been developed to create vertically aligned carbon nanotube (VACNT) thermal interface materials that can be attached to a variety of metallized surfaces. VACNT films were grown on Si substrates using standard CVD processing followed by metallization using Ti/Au. The coated CNTs were then bonded to metallized substrates at 220 °C. By reducing the adhesion of the VACNTs to the growth substrate during synthesis, the CNTs can be completely transferred from the Si growth substrate and used as a die attachment material for electronic components. Thermal resistance measurements using a photoacoustic technique showed thermal resistances as low as 1.7 mm^2 K W^{-1} for bonded VACNT films 25–30 μm in length and 10 mm^2 K W^{-1} for CNTs up to 130 μm in length. Tensile testing demonstrated a die attachment strength of 40 N cm^{-2} at room temperature. Overall, these metallized and bonded VACNT films demonstrate properties which are promising for next-generation thermal interface material applications.

(Some figures in this article are in colour only in the electronic version)

1. Introduction

Considerable attention has been focused on developing advanced thermal interface materials (TIMs) that utilize the extraordinarily high axial thermal conductivity of carbon nanotubes (CNTs). For CNTs, theoretical predictions suggest thermal conductivity values as high as 3000 W m^{-1}K^{-1} [1] and 6600 W m^{-1}K^{-1} [2] for individual multi-wall and single-wall CNTs, respectively. Compared to the thermal conductivity of state-of-the-art thermal interface materials, the axial thermal conductivity of CNTs is at least two orders of magnitude greater. However, the development of carbon-nanotube-based TIMs have yet to produce films which are close to the high thermal conductivity found in individual nanotubes. Early studies focused on dispersing CNTs in a compliant polymer matrix to enhance the effective thermal conductivity of the composite structures [3]. Yet, only modest improvements in thermal performance over neat polymers were achieved. This was a result of the large thermal resistances which exist between CNTs and polymer matrices as well as the reduction in phonon velocities in the CNTs caused by interactions with the polymer matrix [4]. More recently, significant attention has shifted to vertically aligned CNT (VACNT) arrays in the form of films and mats. In contrast to the polymer–CNT composites, the VACNT arrays are promising TIM structures that have demonstrated thermal properties that compare favorably to state-of-the-art TIM materials [5]. VACNT films possess a synergistic combination of high mechanical compliance and high effective thermal conductivity—in the range of 10–200 W m^{-1}K^{-1} [6–8]. The compliance of these films is particularly advantageous in addressing mismatches in coefficients of thermal expansion that can cause TIM

 © 2010 IOP Publishing Ltd Printed in the UK & the USA

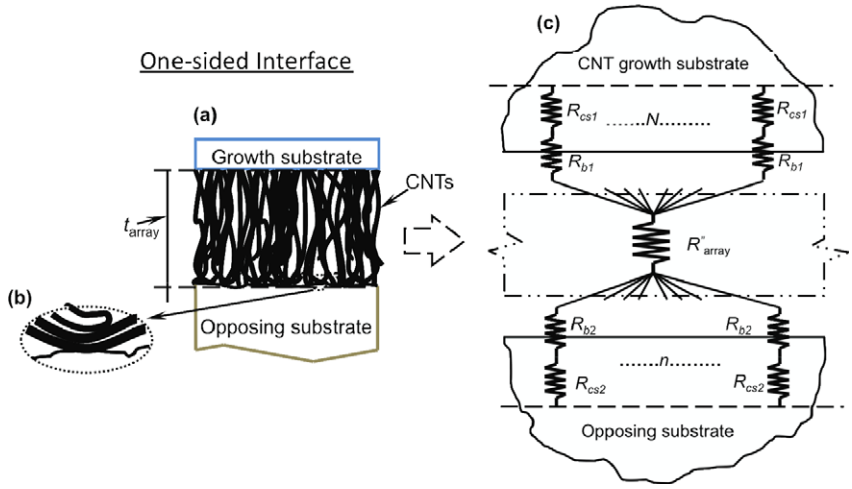

Figure 1. (a) Schematic (not to scale) of an interface with the addition of a vertically oriented CNT array of thickness t_{array} [5]. (b) Buckled CNT contacting an opposing surface with its wall. As shown, some CNTs do not make direct contact with the opposing surface.
(c) Resistance schematic of a one-sided CNT array interface between two substrates, showing constriction resistances (R_{csi}), phonon ballistic resistances (R_{bi}) and the effective resistance of the CNT array (R''_{array}).

delamination and device failure. Also, in contrast to polymer–CNT composites and the best thermal greases, CNT array interfaces are dry and chemically stable in air from cryogenic to high temperatures (∼450 °C), making them suitable for extreme-environment applications [9].

The most actively studied CNT array interface structure is the 'one-sided' CNT array interface that consists of CNTs directly grown on one substrate with the free ends of the CNTs in contact with an opposing substrate (see figure 1). The numerous CNT contacts at both the growth and opposing substrates form parallel heat flow paths within the framework of the thermal resistance network. The resistance at each local CNT–substrate contact can be modeled as two resistances in series [10]: (1) a classical substrate constriction resistance (R_{cs}) and (2) a resistance (R_b) that results from the ballistic nature of phonon transport through contacts much smaller than the phonon mean free path in the materials (∼100 nm). The remaining resistance (R''_{array}) is from heat conduction through the CNT array. This effective resistance is defined for the entire array (including void spaces). Based on previous measurements, when the array height is less than 50 μm, R''_{array} is usually negligible in comparison to the resistances at the CNT–substrate contacts [10]. Thus, the development of high performance thermal interface materials based on VACNTs requires the reduction in contact resistance between CNTs and their mating substrates. Overall, it has been observed that the larger of the two contact resistances exists between the free ends of the CNTs and the opposing substrate when compared to the contact between CNTs and the growth substrate.

The thermal resistance between the opposing substrate and the CNT free ends has been reduced through the application of pressure across the CNT interface. The use of a pressure contact results in increased contact area, providing more parallel pathways for heat to flow into the CNT array. Thus, such contacts heavily depend on the deformation and contact mechanics at the interface. Typical specific thermal resistances, which are normalized based on contact area for these TIMs, lie in the range of 7–20 mm^2 K W^{-1} for contact with surfaces such as Ag, Cu, Ni and Al (table 1). Alternatively, metallization using indium has also been utilized to bond the CNTs to a second substrate, resulting in improved interface resistance without the need for pressure. Resistances for this type of metallization have reached values close to 1 mm^2 K W^{-1}, showing the importance of addressing the contact resistance at the CNT–substrate interface (table 1). Overall, the use of metallization is a promising processing step that may enable the VACNTs to act as a die attachment layer. However, the long term stability issues surrounding the use of indium and other low melting point solder metallizations can limit the application of these TIMs due to degradation of the metallization. Moreover, the mechanical strength of these interfaces has not been tested to determine if they will be sufficient for die attachment. Beyond considerations for metallization, it should be noted that the single-sided CNT interface structure requires synthesis on substrates at elevated temperatures. Due to the high processing temperatures and the potential incompatibility of the catalyst with the growth substrate, this architecture puts limitations on the materials which can be utilized in making VACNT-based TIMs.

In this paper, we explore the use of metallization and bonding of VACNT films for the creation of thermal interface and die attachment materials. The metallization is based on evaporated titanium and gold layers, which are used to bond CNT interfaces at temperatures typical of solder reflow cycles. To circumvent the problems of synthesizing VACNTs on sensitive substrates, a combination of transfer printing and thermocompression bonding [19, 20] was used to transfer CNTs from their growth substrates to bulk copper and Si substrates. Copper and Si were used to represent heat sinks and temperature-sensitive electronic components, which are involved in electronics packaging. Thermal resistance of the entire array was explored using a photoacoustic method [14] while die attachment strength was measured through tensile testing.

Table 1. Thermal resistances of one-sided CNT array TIMs.

Interface	Array height (μm)	Number density (CNTs μm^{-2})	CNT diameter (nm)	Pressure (kPa)	Resistance (mm^2 K W^{-1})
Dry contacts					
Si–CNT–Ag [11]	25	100–1000	20–60	350	7.0 ± 0.5
Si–CNT–Cu [12]	13	30	15–50	450	19 ± 5
Si–CNT–Ni [13]	30	10	100	550	12 ± 1
Si–CNT–Ag [14]	40	100–1000	20–40	210	8.0 ± 0.5
Si–CNT–Al [15]	10	18	10–15	150	7 ± 5
Si–CNT–Ni [16]	45–55	270	—	410	8 ± 1
SiC–CNT–Ag [9]	20–30	100–1000	40	69	12 ± 1 (at 250 °C)
Free ends bonded					
Si–CNT/In–Au [17]	10	100–1000	20–30	—	~1
Si–CNT/Pd–Al [18]	28	87 000	1–2	—	12 ± 1

2. Experimental procedure

2.1. CNT growth

Vertically aligned carbon nanotubes were grown using a thermal chemical vapor deposition (CVD) process in a quartz tube furnace. Synthesis conditions and times were varied in order to produce CNTs, which ranged in length from 20–225 μm. For the growth of CNTs longer than 100 μm in length, first, 100 nm of silicon dioxide was grown on 1 cm × 1 cm silicon substrates using plasma-enhanced chemical vapor deposition. Next, 5 nm of Fe was evaporated onto the oxidized Si wafer to form the catalyst layer for carbon nanotube synthesis. The CVD synthesis of the carbon nanotubes was performed up to 5 min at 800 °C using a combination of argon, hydrogen, methane and acetylene as process gases. At a temperature of 800 °C, CNT array heights up to 225 μm were obtained during the synthesis process. To increase the adhesion of the CNTs to the substrate, a 10 nm thick layer of Ti was applied directly to the Si substrate without the use of SiO_2. Next, a 5 nm Fe layer was evaporated on top of the Ti layer and the same growth procedure as described above was used to synthesize the CNTs. The use of this catalyst layer reduced the growth rate of the CNTs to approximately 6 μm min^{-1} with a typical growth length of 30 μm after 5 min of growth. Overall, the use of either catalyst system was found sufficient to create one-sided CNT structures as shown in figure 1. However, the use of the Ti/Fe catalyst layer was found to be the most robust in terms of CNT adhesion to the growth substrate.

Since the direct synthesis of CNTs is not always possible on temperature-sensitive devices, we investigated a method to transfer the CNTs from their growth substrates at low temperatures. To create VACNT thermal interface materials through transfer printing, the adhesion of the CNTs to the growth substrate was weakened in order to enhance the yield of the transfer process. It has been shown that introducing water vapor via a carrier gas after the growth phase can help to reduce amorphous carbon within the array, etch the end caps of the nanotubes and also etch the CNT/catalyst interface, thereby weakening its bond to the growth substrate [21]. Thus, this technique was implemented for the transfer printing of CNT arrays to both Cu and Si substrates.

To introduce the water vapor, a bubbler apparatus was attached to the growth furnace. Argon was used as the carrier gas and the flow rate was controlled with an external mass flow controller. The water vapor was introduced immediately after the CNT growth phase at a furnace temperature of 800 °C. This step lasted 5 min and the Ar flow rate was varied up to 160 sccm, depending on the initial CNT length. Lower flow rates were used with shorter CNTs while higher flow rates were found to work well with longer CNTs. After water vapor etching, the samples were removed and transfer-printed onto Cu or Si substrates as discussed below. In some cases, CNT arrays were simply attached to polyimide tape after the water vapor etch. This process provided a convenient method to store CNT array samples for bonding at a later time and will be discussed in section 3.

2.2. Bonding and transfer process

In order to bond the vertically aligned CNTs to an opposing substrate, both the substrate and the free ends of the CNTs were metallized. The metallization consisted of 50 nm of Ti followed by 500–1000 nm of Au. This metallization was chosen since it circumvents some of the reliability issues associated with low melting point solders while being amenable to low temperature processing (<300 °C). The use of bonding temperatures less than 300 °C ensures that the processing is compatible with current solder reflow processing temperature limits used in semiconductor manufacturing. Thus, a wide range of substrates and temperature-sensitive devices, which are also metallized, will be compatible with this process. In general, the mechanism for the bonding across the Au–Au interface is not a reflow process. Instead, it is a result of Au–Au self-diffusion. This method of bonding is generally performed in the presence of an applied external load which has been shown to help reduce the temperature at which the bonding occurs or to improve the bond strength at a given temperature.

The metallized CNTs were bonded to copper and Si substrates also coated with Ti/Au metallization layers. Bonding was performed using a Carver benchtop hot press at 220 °C. To bond one-sided interface materials, the metallization was simply applied to the free ends of the CNTs, which were well adhered to their growth substrate.

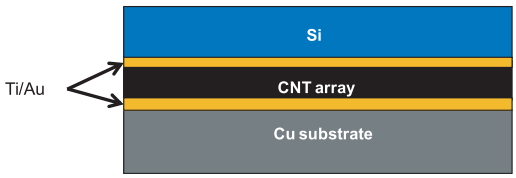

Figure 2. Figure showing structure of samples utilized in the tensile testing of the bonded CNT arrays.

For CNT samples that were exposed to water vapor etching, the bonding process resulted in the complete transfer of the CNT arrays to the Cu or Si substrate. Once transferred, a second metallization layer was applied to the CNTs in order to bond a second substrate, allowing the CNTs to act as a die attachment material. While Ti/Au metallization was used in these experiments, it is also possible to replace the Ti layer with Ni in order to reduce or eliminate the diffusion of metals such as Cu into the gold layer. XPS analysis of thermally annealed samples (240 °C for 10 h) with 100 nm thick Ni layers between the Ti and Au layers have revealed the effectiveness of this diffusion barrier.

2.3. Characterization of the bonded CNT arrays

Tensile testing was utilized to determine the strength of the bonded CNT interfaces. For these experiments, CNT arrays 1 cm × 1 cm in area with an average length of approximately 30 μm were bonded to a copper substrate utilizing the Ti/Au metallization. An additional layer of metallization was then applied to the free ends of the CNTs, which were then bonded to a metallized Si chip, 1 cm × 1 cm in size (figure 2).

The tensile tests were performed using an MTS Insight 2 electromechanical test system equipped with a 100 N load cell and compression platens. Both sides of the sample were attached to self-aligning platens using quick drying glue. Once the adhesive was completely dried, the tensile test was performed at a controlled displacement rate until fracture occurred.

Thermal resistance measurements were performed using a photoacoustic (PA) measurement technique that has been reported previously [14]. The PA technique is a noninvasive procedure that has proven successful at obtaining thermal conductivity of thin films and thermal resistance of interfaces [14]. In the PA technique, a laser heating source was used to periodically irradiate the sample surface, which was surrounded by a sealed acoustic chamber. The acoustic response of the air in the chamber above the sample was measured with a microphone that was embedded in the chamber wall. The measured pressure signal was used in conjunction with the model described in [14] to determine thermal interface resistance. The transient nature of the PA technique and the analysis of many heating frequencies in a single experiment facilitates the good resolution of thermal interface resistance (0.5 mm^2 K W^{-1}) that is necessary to measure structures with low resistance.

In these experiments, both long and short CNTs were measured. For short CNTs, the one-sided thermal interface structure was tested using nanotubes approximately 25–30 μm in length (figure 3). For long CNTs approximately 130 μm in length, the arrays were transfer-printed onto Si substrates since the absence of the Ti layer resulted in poor adhesion to the Si growth substrate, which compromised the PA experiments (figure 3). A 25 μm thick silver foil (99.998%, Alfa Aesar, Inc.) was attached to the top of each sample. The low thermal resistance of the silver foil facilitated increased sensitivity to interface resistance during PA measurements. The Ag film was coated with 80 nm of titanium via electron beam deposition and bonded to the Au-coated CNT arrays at 220 °C. Helium was used as the gas medium for the measurements, as opposed to air or nitrogen, because of its higher thermal conductivity, thus producing the best signal-to-noise ratio.

3. Results

3.1. Synthesis results

The synthesis of the CNTs resulted in dense vertically aligned growth as anticipated and verified through measurements using a Hitachi 3500 scanning electron microscope (SEM). Images revealed CNTs with an average diameter of 18 nm, indicative of multiwall CNTs and a volume fraction of 9%. Additional analysis of the CNTs was performed using Raman spectroscopy using the 488 nm line of an Ar^+ laser, measuring the ratio of the graphitic to defect peak intensities. The G, or graphitic, peak which lies around 1580 cm^{-1} is an indicator of the structural order of the CNTs [22]. The D or defect peak lies around 1380 cm^{-1} and is representative of the disorder present in the CNTs. The ratio of these two peaks is commonly used to assess the quality of CNTs. Raman analysis of the samples showed a graphitic to defect intensity ratio of 1.43 which indicated good structural order for the CNTs (figure 4). Upon exposure to the water vapor etch step, the CNT lengths were reduced, depending on the flow rate used during the 5 min etch step. Data taken from the SEM images showed an etch rate of 400 nm min^{-1} for flow rates as low as 80 sccm and increased up to 16 μm min^{-1} for flow rates of 160 sccm. Negligible etching was observed at Ar–H_2O flow rates as low as 40 sccm. Additional Raman analysis after the etch step showed negligible changes in the ratio of the graphitic to defect (G/D) peak intensities for flow rates up to 40 sccm, maintaining a value of 1.43. Increasing the flow rate above 40 sccm resulted in a linear reduction in the G/D peak with increasing flow rate. However, this ratio remained above 1.3 for flow rates up to 160 sccm tested in this study. These results indicate that relatively good structural order is maintained in the CNTs after the etch step, which is desired for maintaining high thermal conductivity in the CNT array.

To assess the effect of the water vapor etch step on the adhesion of the CNTs to the growth surface, samples with varying Ar–H_2O etch flow rates but a fixed etch time (5 min) were prepared. Polyimide tape was used to attempt to remove the CNTs from the growth surface after etching to assess the ease of transfer. For flow rates from 0–40 sccm, no transfer from the Si growth substrate was observed (figure 5). For flow rates between 40 and 80 sccm, only partial transfers were seen.

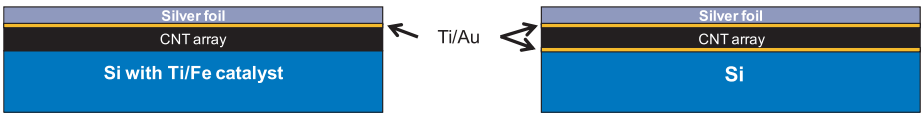

Figure 3. Images showing the structure of the samples used in the PA testing. Left: sample used to measure short CNT arrays (∼30 μm in height). Samples were directly grown on the Si substrate using Ti/Fe catalyst. Right: sample used to measure long CNTs (∼130 μm in height). Samples were transferred and bonded to Si substrates using Ti/Au bonding. For both samples, a 25 μm thick Ag foil was bonded to the top of the array.

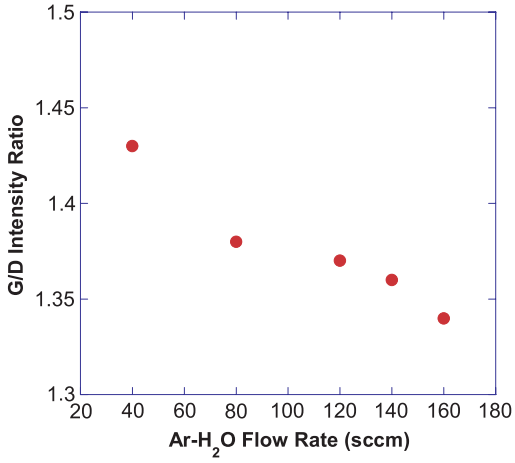

Figure 4. Data showing the ratio of the intensities of the Raman peaks for the G and D bands for CNT arrays as a function of Ar–water vapor flow rate. Data show a clear decrease in the G/D intensity ratio with increasing etchant flow rate, indicating the introduction of an increasing number of defects into the CNT array.

Finally, for flow rates that exceeded 80 sccm, it was found that complete transfers could be obtained. Thus, water vapor etching with Ar–water vapor flow rates of 80 sccm or greater was used to create samples that required transfer printing of the CNTs. As a result of the weak adhesion which occurred during the etch step, complete CNT arrays could be removed from the growth substrate simply by using polyimide tape and stored for later use in the transfer printing and bonding process (figure 6). While these results were found using polyimide tape, the results were similar to those seen in the transfer printing process.

Figure 6. Picture showing the transfer of 1 cm × 1 cm VACNT arrays to polyimide tape. The ease of transfer was aided by etching the nanotubes using an Ar–H_2O flow rate of 80 sccm.

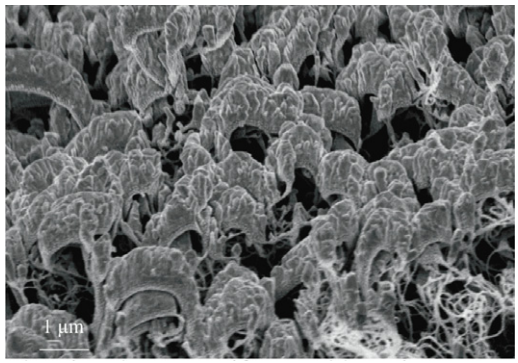

Figure 7. SEM image showing the non-uniform gold coating on top of the CNT array, forming large particles on the tops of CNTs.

3.2. Metallization and bonding

The metallization of the CNT arrays was analyzed using optical and scanning electron microscopy as shown in figure 7. The metallization thickness was measured during e-beam evaporation using a quartz crystal microbalance. Thus, the 500 nm thick Au layer measured during deposition is based

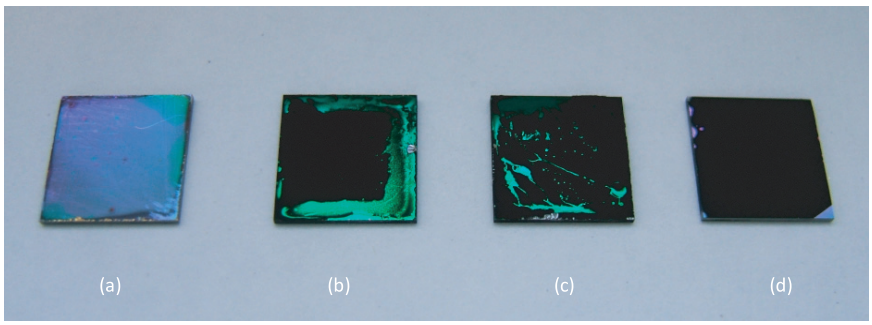

Figure 5. Examples of CNT growth substrate after attempts to transfer CNTs to polyimide tape. The left sample shows complete transfer of CNTs after an 80 sccm Ar–H_2O etch flow rate. The middle two samples show partial transfers using 60 sccm and 50 sccm, respectively. The right sample (d) utilized a 30 sccm flow rate and displayed no CNT transfer.

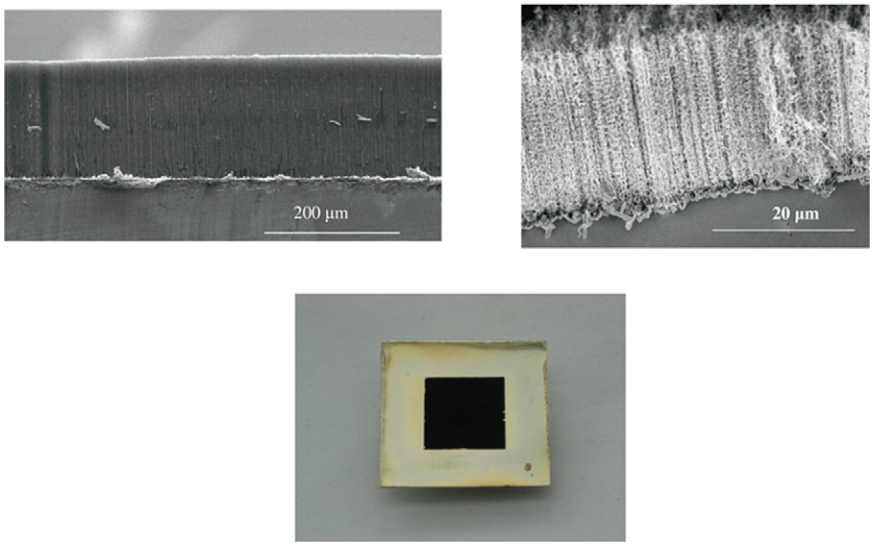

Figure 8. Images showing the transfer of VACNT to metallized substrates: (top left) 200 μm long CNTs transferred to Si; (top right) 25 μm long CNTs transferred to Si, and (bottom) 30 μm long CNTs transferred to Cu.

on assuming a continuous film whereas the SEM image clearly shows that the metallization is discontinuous. The metallization formed large and small clumps on many of the tubes in the array. Since the coating is not uniform over the CNT array, as shown in figure 7, this may indicate that any interface bonded with this metallization could have a pressure-dependent thermal resistance. This pressure dependence will arise from the fact that the CNTs with thick metallization may contact and bond at the interface prior to CNTs which have little or no metallization. Thus, applied pressure will help to increase the contact area at the bonded interface if all CNTs are not attached during the initial bonding procedure. As a result, the pressure dependence of the thermal resistance was tested in this study.

The results of the transfer printing procedure are shown in figure 8. In this figure, both long and short CNTs were transferred to Si and Cu substrates. It is clear that the VACNT arrays retain their vertical alignment, which is important for creating interface materials. In addition, the weak interface to the growth substrate promoted by the etch step allowed easy removal of the growth substrate which was simply pulled off by hand after the bonding step. The use of bonding temperatures between 150–220 °C all resulted in successful transfers to these secondary substrates, providing a low temperature processing window for creating CNT thermal interface and die attachment materials. However, it is not believed that melting and Au reflow at the interface are responsible for the successful bonding of the Au interfaces. While the use of small metal particles has been shown to reduce the melting temperature of Au, this phenomena typically happens for particles with diameters less than 100 nm. Based on the metallization particles seen in figure 7, no suppression of the melting temperature is believed to occur during the bonding process. However, the bonding across the interface is believed to be aided by the rapid diffusion of Au and Cu atoms across the interface, which can aid in the formation of bonding at low temperatures. After transferring the CNTs to the Si or Cu substrates, a second layer of Ti/Au metallization was applied to the free ends and a second substrate was bonded to the VACNT array. The results of this process are shown in figure 9 where 1 cm × 1 cm Si chips are attached to Cu substrates through the use of metallized VACNT arrays.

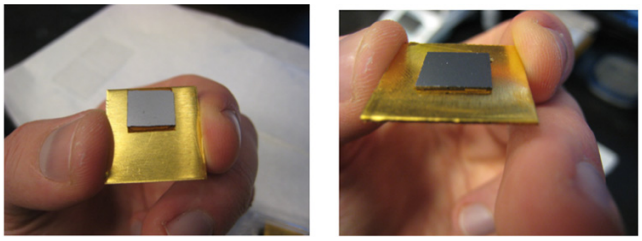

Figure 9. Image showing the attachment of an Si chip to a Cu substrate by bonding to metallized VACNT arrays.

As previously mentioned, the VACNT arrays could be attached to polyimide tape and stored for later use. Polyimide tape was chosen due to its compatibility with the bonding temperatures used in the process described here. After applying the Ti/Au metallization layer to the VACNT arrays on the polyimide tape, the samples were placed in the Carver hot press and bonded to metallized substrates as previously described, resulting in a successful bond. Removal of the polyimide tape was performed by soaking the sample in acetone, which removed the adhesive and the polyimide backing film. This process thus demonstrates the ability to store, handle and process VACNT arrays from high temperature tapes, which can be important for scaling up the manufacturability of this process.

3.3. Mechanical and thermal characterization results

3.3.1. Mechanical test of bond strength. Mechanical testing was performed on Si samples bonded to Cu substrates using the metallized CNTs (figure 10). Data show very good

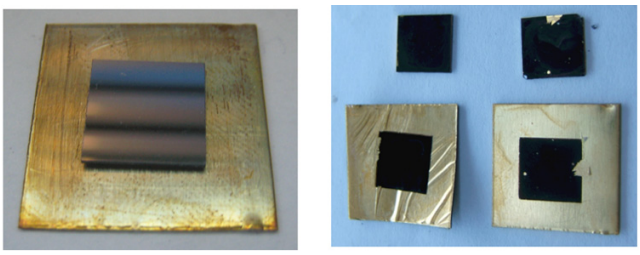

Figure 10. Optical images of the tensile testing of 1 cm × 1 cm Si chips bonded to copper substrates using metallized CNTs (left) and an image showing failed samples which display nearly uniform coverage of CNTs on both surfaces (right).

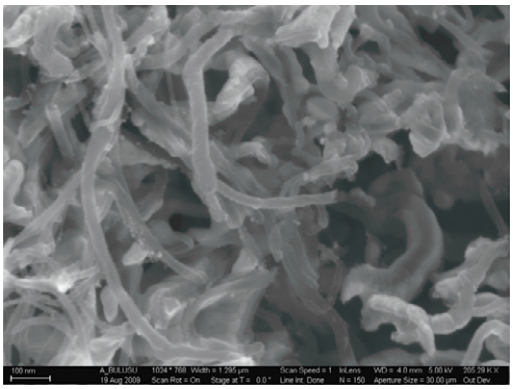

Figure 11. High resolution SEM showing broken fibers embedded in Au that were observed after tensile testing. These images indicate that the failure occurs due to CNT fracture.

bond strengths for the low temperature bonding, with failure occurring at loads between 35 and 40 N cm^{-2}. Examination of the failed samples clearly showed that nearly uniform coverage of CNT layers was present on each substrate. Further examination of the interface using a high resolution scanning electron microscope showed clearly that some of the CNTs embedded in the Au bond layer were broken (figure 11). While it cannot be ruled out that CNT pull out occurred, these images show that part of the failure mechanism is clearly CNT fracture. Thus, the strength and density of the CNTs will limit the overall strength of the CNT die attachment layers. Previous reports on the strength of anodically bonded CNT interfaces have shown strengths of the order of 4.3 N cm^{-2} [23]. However, in the case of the metallized and bonded samples presented here, the strength of the interface is nearly an order of magnitude larger, showing the effectiveness of the bond.

3.3.2. CNT interface resistance from PA measurement technique. The resistance for one-sided interface and transferred VACNT arrays as shown in figure 3 were tested using the PA technique. The pressure dependence of this resistance was also measured to account for the non-uniform metallization layers on the CNTs. As previously mentioned, the application of pressure could possibly bring more CNTs into contact with the interface as a result of the metallization structure, thereby reducing the overall thermal resistance.

The results of the PA tests are shown in table 2. It should be noted that here we only report the total thermal contact resistance and make no attempts to separate out the resistance for the CNTs and each bonded interface. For the one-sided interface with CNTs of the order of 25 μm in length, the overall resistance of the array was shown to be 4.5 mm^2 K W^{-1} without any applied pressure. This resistance compares favorably with high performance solder interfaces [24], showing the effectiveness of the Ti/Au layer metallization and bonding. A reduction to 1.7 mm^2 K W^{-1} was achieved with an applied pressure of 69 kPa. Again, this value shows excellent performance of the interface material. However, it also indicates that increased CNT interface contacts can be made with applied pressure in spite of the applied metallization. Thus, the continued development of such interfaces must address the effective contact with the maximum number of CNTs in the array in order to improve the overall thermal resistance.

Table 2. Thermal resistance results.

Sample	Thermal resistance (mm^2 K W^{-1})
One-sided interface, 30 μm long	4.5 ± 0.5
One-sided interface, 30 μm long, 69 kPa pressure	1.7 ± 0.5
Transfer-printed, 30 μm long	10 ± 0.5
Transfer-printed, 130 μm long	10 ± 0.5

For the transferred and bonded CNT array, both long (130 μm) and short (30 μm) CNTs were measured as seen in table 2. The thermal resistance of the long CNT array was found to be 10 mm^2 K W^{-1} with no applied pressure. For the short CNT array, again the overall thermal resistance was found to be 10 mm^2 K W^{-1}. The independence of the thermal resistance to the CNT length suggests that the interface resistance at the two bonded interfaces in the transferred samples dominates the overall resistance of the structure. Again, improvements in the metallization and contacts during the bonding process may enable a lowering of the overall resistance of the array.

4. Conclusions

The use of Ti/Au metallization is an effective method for creating thermal interface materials using vertically aligned carbon nanotubes. Ti/Au is effective since it provides the ability to create low temperature diffusion bonds which are amenable to die attachment thermal processing temperatures currently found in semiconductor device packaging. Through the use of a water vapor etch step after the growth phase, the CNT arrays can be easily transfer-printed from the growth substrate to a wide range of metallized substrates. This method effectively separates the high temperature synthesis from the low temperature tolerances typically observed with most heat spreaders and electronic devices. Thermal interface resistances showed that values of the order of 10 mm^2 K W^{-1} could be obtained with transfer-printed CNTs. This value was found not to vary when comparing CNTs 30 and 130 μm in length. This indicates that the interface resistance and not the bulk resistance of the CNTs governs the overall resistance in these

samples. For single-sided interfaces, a lower thermal resistance was found, of the order of 4.5 mm^2 K W^{-1}. This value is around 50% of the transfer-printed CNTs. Since the single-sided interfaces has one bonded interface as opposed to two, this again points to the inherent resistance at the interface governing the overall resistance of the thermal interface material. It should be noted that the Ti/Fe shows less thermal resistance than the Ti/Au interface. This is due to the fact that the CNTs are nucleated from the Ti/Fe during growth and a high percentage of them are inherently connected to the Ti/Fe metallization on the substrate. On the other hand, the evaporated Ti/Au coats the CNT array, but does not guarantee that all CNTs are inherently connected to the Au metallization. Thus, the issue of addressing contact resistance at the interface is related to the ability to form connections with as many CNTs in the array as possible. Due to the fact that a pressure-dependent contact resistance is observed in the Ti/Au metallized CNT arrays, it is a clear indication that not all CNTs in the array are in connection with the bonded Ti/Au surface. As the array is pressed, more of the CNTs come into contact, thus reducing the thermal resistance. Therefore, the maximum benefit in creating the CNT thermal interface materials will be based on techniques which can maximize the number of contacts at each interface.

References

[1] Che J, Cagin T and Goddard W A 2000 Thermal conductivity of carbon nanotubes *Nanotechnology* **11** 65–9

[2] Berber S, Kwon Y-K and Tomanek D 2000 Unusually high thermal conductivity of carbon nanotubes *Phys. Rev. Lett.* **84** 4613–6

[3] Biercuk M J, Llaguno M C, Radosavljevic M, Hyun J K, Johnson A T and Fischer J E 2002 Carbon nanotube composites for thermal management *Appl. Phys. Lett.* **80** 2767–9

[4] Prasher R 2007 Thermal conductance of single-walled carbon nanotube embedded in an elastic half-space *Appl. Phys. Lett.* **90** 143110

[5] Cola B A, Fisher T S and Xu X 2009 *Carbon Nanotubes: New Research* ed A P Ottenhouse (New York: Nova Science Publishers) pp 101–18

[6] Hu X J, Padilla A A, Xu J, Fisher T S and Goodson K E 2006 3-omega measurements of vertically oriented carbon nanotubes on silicon *Trans. ASME, J. Heat Transfer* **128** 1109–13

[7] Yang D J, Zhang Q, Chen G, Yoon S F, Ahn J, Wang S G, Zhou Q, Wang Q and Li J Q 2002 Thermal conductivity of multiwalled carbon nanotubes *Phys. Rev.* B **66** 165440

[8] Hone J, Llaguno M C, Nemes N M, Johnson A T, Fischer J E, Walters D A, Casavant M J, Schmidt J and Smalley R E 2000 Electrical and thermal transport properties of magnetically aligned single wall carbon nanotube films *Appl. Phys. Lett.* **77** 666–8

[9] Cola B A, Capano M A, Amama P B, Xu X and Fisher T S 2008 Carbon nanotube array thermal interfaces for high-temperature silicon carbide devices *Nanos. Microsc. Thermophys. Eng.* **13** 228–37

[10] Cola B A, Xu J and Fisher T S 2009 Contact mechanics and thermal conductance of carbon nanotube array interfaces *Int. J. Heat Mass Transfer* **52** 3490–503

[11] Cola B A, Amama P B, Xu X and Fisher T S 2008 Effects of growth temperature on carbon nanotube array thermal interfaces *Trans. ASME, J. Heat Transfer* **130** 114503

[12] Xu J and Fisher T S 2006 Enhanced thermal contact conductance using carbon nanotube array interfaces *IEEE Trans. Compon. Packag. Technol.* **29** 261–7

[13] Xu Y, Zhang Y, Suhir E and Wang X 2006 Thermal properties of carbon nanotube array used for integrated circuit cooling *J. Appl. Phys.* **100** 074302–5

[14] Amama P B, Cola B A, Sands T D, Xu X and Fisher T S 2007 Dendrimer-assisted controlled growth of carbon nanotubes for enhanced thermal interface conductance *Nanotechnology* 385303

[15] Zhang K, Chai Y, Yuen M M F, Xiao D G W and Chan P C H 2008 Carbon nanotube thermal interface material for high-brightness light-emitting-diode cooling *Nanotechnology* 215706

[16] Liu X, Zhang Y, Cassell A M and Cruden B A 2008 Implications of catalyst control for carbon nanotube based thermal interface materials *J. Appl. Phys.* **104** 084310

[17] Tong T, Yang Z, Delzeit L, Kashani A, Meyyappan M and Majumdar A 2007 Dense vertically aligned multiwalled carbon nanotube arrays as thermal interface materials *IEEE Trans. Compon. Packag. Technol.* **30** 92–100

[18] Panzer M A, Zhang G, Mann D, Hu X, Pop E, Dai H and Goodson K E 2008 Thermal properties of metal-coated vertically aligned single-wall nanotube arrays *Trans. ASME, J. Heat Transfer* **130** 052401

[19] Allen A C, Sunden E, Cannon A, Graham S and King W 2006 Nanomaterial transfer using hot embossing for flexible electronic devices *Appl. Phys. Lett.* **88** 083112

[20] Sunden E, Moon J K, Wong C P, King W P and Graham S 2006 Microwave assisted patterning of vertically aligned carbon nanotubes onto polymer substrates *J. Vac. Sci Technol.* B **24** 1947–50

[21] Zhu L, Xiu Y, Hess D W and Wong C-P 2005 Aligned carbon nanotube stacks by water-assisted selective etching *Nano Lett.* **5** 2641–5

[22] Jorio M A P A, Souza Filho A G, Saito R, Dresselhaus G and Dresselhaus M S 2003 Characterizing carbon nanotube samples with resonance Raman scattering *New J. Phys.* **5** 17

[23] Aradhya S V, Garimella S V and Fisher T S 2008 Electrothermal bonding of carbon nanotubes to glass *J. Electrochem. Soc.* **155** K-161–K-5

[24] Samson E C, Machiroutu S V, Chang J-Y, Santos I, Hermerding J, Dani A, Prasher R and Song D W 2005 Interface material selection and a thermal management technique in second-generation platforms built on intel centrino mobile technology *Intel Technol. J.* **09** 75–86